JOURNAL OF CATALYSIS 96, 586–596 (1985)

Spectroscopic Study of the Ammonia–CO and Pyridine–CO Interaction on MgO–CoO Solid Solutions

A. ZECCHINA AND G. SPOTO

Istituto di Chimica Fisica, Università di Torino, Corso M. d'Azeglio 48, 10125 Torino, Italy

Received September 18, 1984; revised February 15, 1985

Ammonia and pyridine (Py) are adsorbed both dissociatively and nondissociatively on dilute MgO–CoO solid solutions. As on pure MgO, the dissociative process occurs mainly on cobalt-free parts of the surface, with formation of NH_2^- and bipyridyl and pyridine radical anions. Radical species formed in the proximity of Co^{2+} ions are oxidized to neutral bipyridyl. The interaction of CO with NH_2^- and molecularly adsorbed NH_3 gives adsorbed $HCONH^-$ species, preferentially located on the MgO matrix. $HCONH^-$ species located in the proximity of Co^{2+} ions are oxidized to NCO^- with simultaneous formation of $Co(CO)_4^-$ species. A similar redox process occurs with Py, with formation of neutral bipyridyl and $Co(CO)_4^-$.

INTRODUCTION

The surface chemistry of MgO–CoO solid solutions has received much attention in the past (Ref. (*1*) and references therein). Recent results obtained by combined use of IR and UV–visible reflectance spectroscopy (*1*) have shown that CO interacts at room temperature (RT) with isolated Co^{2+} and O^{2-} clusters present in very exposed (coordinatively unsaturated: cus) situations giving $[(CO)Co(CO_2)_2]^{2-}$ and $[Co(CO)_3]^{2+}$ species. At 77 K also the Co^{2+} ions present on the {100} faces interact with CO giving linear $L_5\,Co^{2+}CO$ ($L = O^{2-}$ ions of the surface and the bulk) adducts. RT interaction of CO with clustered $(Co^{2+}O^{2-})_n$ groupings results in a slow reduction process and formation of carbonate-like (oxidized) and $Co(CO)_4^-$ (reduced) species.

$Co^{2+}O^{2-}$ pairs present on edges and steps split hydrogen in a heterolytic way (*2*) with formation of surface hydrides and hydroxyls.

Finally, Co^{2+} ions emerging on the surface form with O_2 a variety of $Co^{3+}O^{2-}$ superoxo complexes which are both IR (*3*) and EPR active (*4*).

In order to extend the knowledge of the surface chemistry of these mixed oxides, in this investigation the adsorption of basic molecules is studied together with their interaction products with CO.

EXPERIMENTAL

MgO–CoO solid solutions containing variable molar fractions of CoO have been prepared according to Ref. (*1*). In this study a dilute solid solution containing 3.4% of cobalt atoms ($Mg_{1-x}Co_xO$, $x = 0.034$), designated MC 3.4, has been mainly used (specific surface area 150–180 $m^2\,g^{-1}$). The cleaning of the surface from all adsorbed species has been obtained by outgassing under high vacuum (10^{-5} Torr; 1 Torr = 133 N m^{-2}).

The gases (NH_3 and CO) were of high-purity grade (Matheson). Pyridine (Py) was purified by the freeze–pump–thaw technique and dosed as vapor.

IR spectra have been taken on a Perkin–Elmer PE 580B spectrometer equipped with a data station; UV–vis reflectance spectra were obtained with a Beckman DK2 instrument by using a suitable all-silica reflectance cell. Gravimetric determinations of the NH_3 coverage at various pressures were obtained with a Sartorius microbalance.

0021-9517/85 $3.00

RESULTS

1. The Spectra of Adsorbed NH_3 and Py

In Fig. 1, the IR spectra of NH_3 adsorbed on a totally dehydroxylated MC 3.4 surface taken at various equilibrium pressures are illustrated.

As already observed on pure MgO (*5*) three main and complex absorptions are present in the ranges 3750–2900, 1650–1550, and 1150–800 cm^{-1} when NH_3 is dosed (p = 50 Torr, coverage θ = 0.2). The peaks at 3745, 3583, and 935 cm^{-1} are fairly insensitive to pressure changes at RT; on the contrary the other bands are severely influenced, so indicating that they belong to weakly bonded species (vide infra).

By reducing the NH_3 pressure from 50 to 5 Torr (θ = 0.13) the components at 3307 and 3217 cm^{-1} disappear, leaving three weaker bands at 3425(sh), 3330, and 3225 cm^{-1}. Further pressure reduction to 5 × 10^{-2} Torr (θ = 0.1) weakens also this triplet, leaving a doublet at 3335 and 3250 cm^{-1}.

Also the absorption at 1650–1550 cm^{-1} is composite; in fact, it is the superposition of three components at ~1625(sh), 1598, and 1550 cm^{-1}. By reducing the NH_3 equilibrium pressure from 50 to 5 Torr the shoulder disappears; further pressure reduction down to 5 × 10^{-2} Torr causes preferential destruction of the component at 1598 cm^{-1}. Upon reduction of the NH_3 pressure from 50 to 5 Torr a component at 1015 cm^{-1} readily disappears leaving two bands at 1040 (narrow) and 1080 cm^{-1} (broader). Further pressure reduction causes a gradual reduction of their intensity and a continuous upward shift of their frequency ($\Delta\bar{\nu}$ = 25 and 22 cm^{-1}, respectively), the high-frequency component showing an increasing resistance to evacuation.

On the basis of the described behavior, the various components can be associated with different surface species as schematically reported in Table 1.

The spectra reported in Fig. 1 are practically identical to those observed for the MgO–NH_3 system (*5*). This could mean that (i) the Co^{2+} ions emerging on the sur-

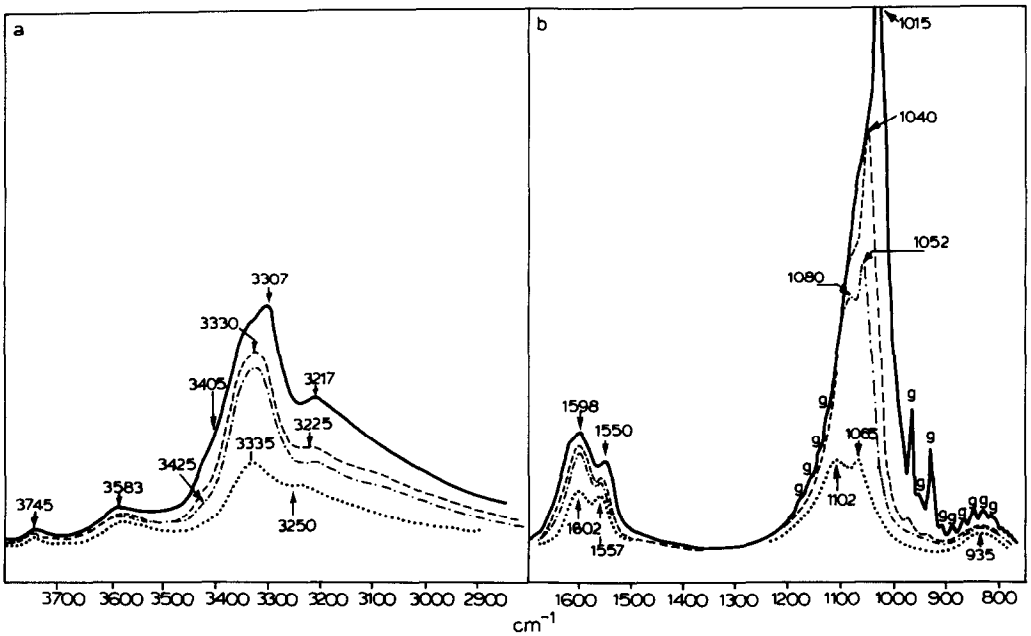

FIG. 1. IR spectra of NH_3 adsorbed on MgO–CoO (3.4% Co, MC 3.4) solid solution, at decreasing equilibrium pressures. (—) 50 Torr; (---) 5 Torr; (-·-·) 1 Torr; (···) 5 × 10^{-2} Torr (g stands for gas-phase bands).

TABLE 1

IR Bands (cm^{-1}) of the Adsorbed NH_3 Species

Very weakly adsorbed	Weakly adsorbed	Strongly adsorbed
3307	3330	3335
3217	3225	3250
1625	1598–1602	1557–1550
1015	1040–1065	1102–1080

face do not participate in the NH_3 chemisorption process; (ii) the IR features of NH_3 adsorbed on Co^{2+} ions and/or $Co^{2+}O^{2-}$ pairs are not appreciably different from those of the NH_3 adsorbed on Mg^{2+} and $Mg^{2+}O^{2-}$ pairs and are thus buried in the strong absorption of NH_3 adsorbed on the matrix.

In order to ascertain if the Co^{2+} ions are active in NH_3 chemisorption, the effect of NH_3 adsorption on the *d–d* spectrum of surface Co^{2+} ions is illustrated in Fig. 2a. It can be seen that (i) the peaks at ~17,000 and 4500 cm^{-1} (and ascribed to *d–d* transitions of fourfold coordinated ions on edges and steps) (*1*) are destroyed; (ii) the main peaks at 19,230, 18,250, 16,530, 13,800, and 7000 cm^{-1} (assigned to *d–d* transitions of Co^{2+} ions in square pyramidal C_{4v} geometry of the {100} faces) (*1*) are only marginally perturbed; (iii) two weak and narrow peaks at 4950 and 4250 cm^{-1} grow in intensity.

The continuous frequency shift clearly observed for the 1080- and 1040-cm^{-1} bands implies that each adsorbed species induces continuous spectral modifications on the other ones adsorbed in adjacent and more distant positions. In order to obtain information about the nature of this effect and contemporarily to investigate the role of Co^{2+} in H–D exchange, the IR spectra in the range 1200–1800 cm^{-1} of NH_3–ND_3 mixtures (9 : 1, 1 : 1, 1 : 9) adsorbed on the MC 3.4 solid solution are compared (Fig. 3a). The spectra are very complex; however (as far as the range 1250–800 cm^{-1} is concerned), they can be interpreted in terms of 7 main components at 1232, 1178, 1150, 1030, 960, 875, and 810 cm^{-1} (Table 2). In the spectrum of the 1 : 1 mixture, the 960- and 875-cm^{-1} bands are the main components, while those at 1030 and at 810 cm^{-1} (which are the main peaks of the 9 : 1 and 1 : 9 mixtures) are much less intense.

The effect of decreasing the NH_3 equilibrium pressure is shown in Fig. 3b (1 : 1 mixture) and Fig. 3c (1 : 9 mixture). The peaks at 960 and 875 cm^{-1} reveal a doublet structure (similar to that of the 1030-cm^{-1} absorption of adsorbed NH_3), each component undergoing a continuous upward frequency shift (as $\theta \rightarrow 0$) identical to that already observed for the equivalent peaks of adsorbed NH_3.

It is thus concluded that the continuous

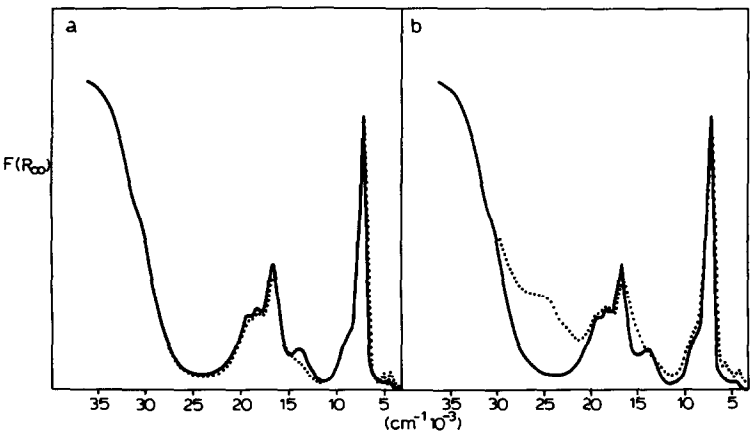

FIG. 2. UV–Visible reflectance spectra of MC 3.4 solid solution before (—) and after adsorption of (a) NH_3 and (b) Py (···).

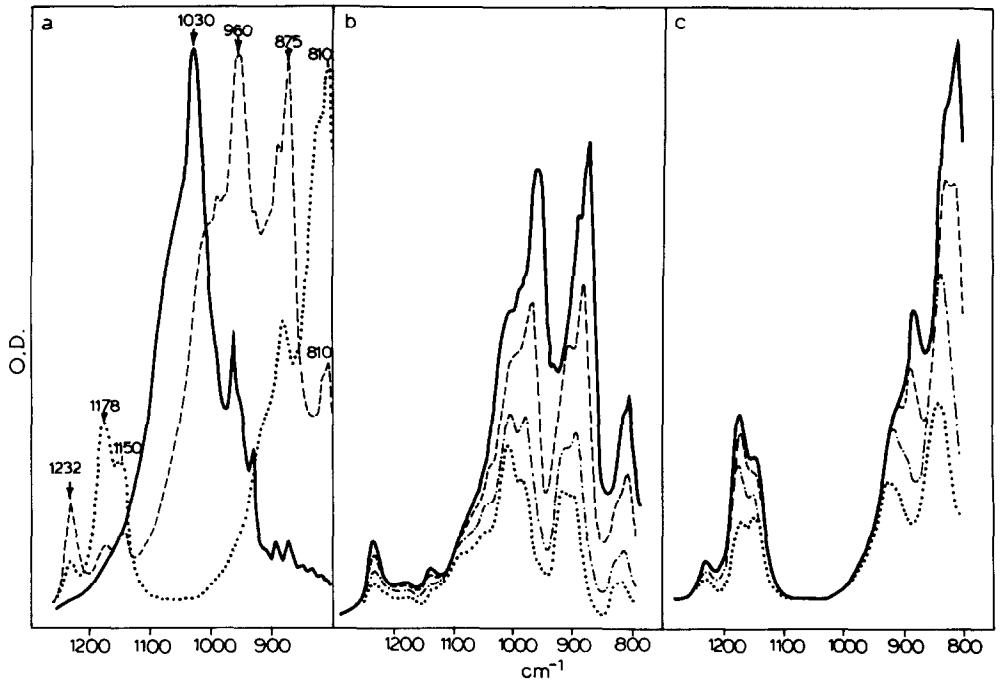

FIG. 3. (a) IR spectra of NH_3–ND_3 mixtures adsorbed on MC 3.4 solid solution (equilibrium pressure: 4 Torr). (—) 9/1; (---) 1/1; (···) 1/9. (b) Effect of decreasing the equilibrium pressure on the IR spectrum of the 1/1 mixture. (c) Effect of decreasing the equilibrium pressure on the IR spectrum of the 1/9 mixture.

positive shift as $\theta \rightarrow 0$ of the bands of adsorbed NH_3, ND_3, and other isotopic species (ND_2H and NHD_2; vide infra) is only influenced by coverage changes and does not depend upon the isotopic composition.

The IR spectrum of adsorbed Py (range 2000–800 cm^{-1}) is reported in Fig. 4a (full line); it is very similar to that observed for the Py–MgO system and its full description and discussion will consequently be given elsewhere (*6*). In this paper we stress only that it strongly resembles that of Py coordinated to Lewis centers (i.e., forming σ-adducts) (*7*), the only important difference being represented by the extra peak at 955 cm^{-1}.

Unlike the Py–MgO system, if Py is left to stand in contact with the surface for several hours, OH stretching bands in the range 3700–3400 cm^{-1} gradually develop, thereby indicating that a dissociative process slowly occurs involving the CH bonds of the Py.

Due to similarity of the IR spectrum of

TABLE 2

IR Bands (cm^{-1}) of Adsorbed NH_3–ND_3 Mixtures

Mixture NH_3 : ND_3	Components						
9 : 1	—	—	—	1030(s)	960(w)	—	—
1 : 1	1232(m)	1178(w)	1150(x)	(1030)(w)	960(s)	875(s)	(810)(w)
1 : 9	1232(w)	1178(m)	1150(m)	—	—	875(w)	(810)(s)

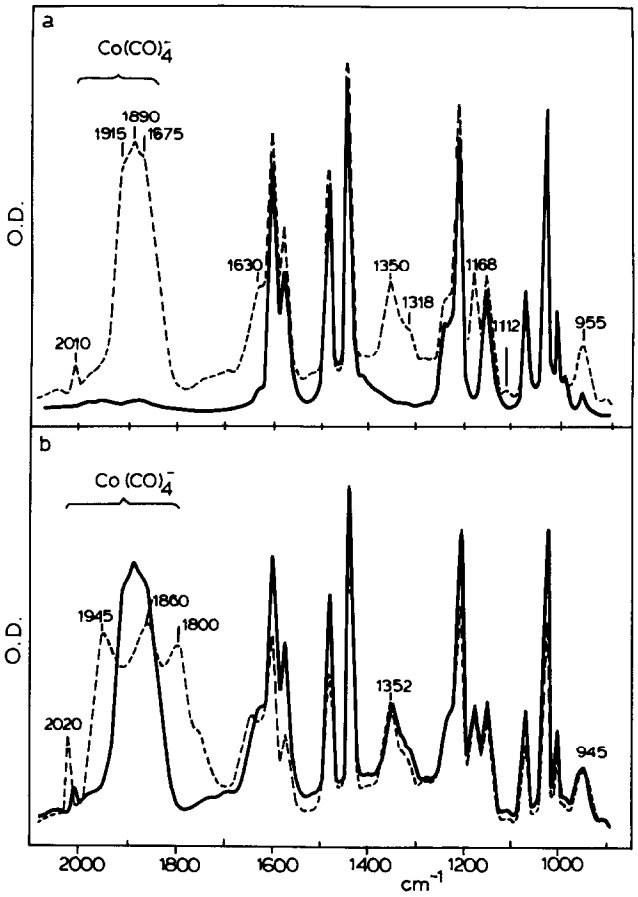

FIG. 4. (a) (—) IR spectrum of adsorbed pyridine on MC 3.4 solid solution (0.1 Torr); (---) after dosing 40 Torr CO. (b) (—) The same as in (a); (---) after outgassing at room temperature.

Py adsorbed on pure MgO and on MgO–CoO dilute solid solutions, it is concluded that the Py probe is not able to distinguish (through its IR spectrum) σ-adducts formed on Mg^{2+} and Co^{2+} ions. However, the active participation of some Co^{2+} ions of the surface in the chemisorption process is demonstrated by the reflectance spectra.

As seen from Fig. 2b (i) the peak at 13,800 cm^{-1} is totally eroded upon Py adsorption; (ii) the peaks at 16,530 and 7000 cm^{-1} are weakened and slightly shifted to lower frequencies. A broad band also gradually develops at 24,000 cm^{-1}, together with weaker features at 5800, 5200, and 4100 cm^{-1}.

2: *The Spectra of the NH_3–CO Interaction Products*

When CO is dosed on preadsorbed NH_3 ($\theta \simeq 0.1$), the spectra illustrated in Fig., 5a are obtained. It can be seen that (i) the adsorbed NH_3 is readily consumed (as monitored by the disappearance of the 1100–1040 and 3330 cm^{-1} absorptions (spectrum a); (ii) new bands are formed at 3700, 3460, 3400, 3345, 2960, 2825, 2730, 2204, 2040, 1940, 1910, 1890, 1610, 1410, 1375, and 1175 cm^{-1} (spectrum b).

If a NH_3–CO mixture (1 : 1; p = 5 Torr) is directly allowed on the surface and left to stand for several hours, the intense spec-

trum c is obtained, which can be considered as the superposition of an intensified spectrum b and the spectrum of unreacted (weakly adsorbed) NH_3.

Successive evacuation of the gas phase allows one to remove the weakly adsorbed NH_3 (bands at ~3350 and at 1080–1020 cm^{-1}) and to obtain the IR spectrum of the NH_3–CO interaction products (with their maximum intensity) (Fig. 5b) in the absence of any "solvent" effect due to the presence of molecularly adsorbed NH_3.

Besides the disappearance of the unreacted NH_3 bands, important modifications of the spectrum of the remaining species occur. In particular: (i) the doublet at 2805 and 2825 cm^{-1} becomes a single band at 2838 cm^{-1}; (ii) the bands at 2990 and 2700 cm^{-1} move downward and upward, respectively ($\Delta\bar{\nu}$ = −35 and +30 cm^{-1}); (iii) the peaks at 2204 and 2040 cm^{-1} become sharper and shift slightly to lower frequency; (iv) the components of the triplet originally observed at 1940, 1910, and 1890 cm^{-1} show a larger separation between the peaks (maxima at 1950, 1850, and 1785 cm^{-1}); (v) the bands at 1400 and 1360 cm^{-1} move upward (+10 cm^{-1}) and downward (−8 cm^{-1}), becoming more intense.

The original spectrum can be completely restored by redosing NH_3 on the surface; consequently, these effects are induced by

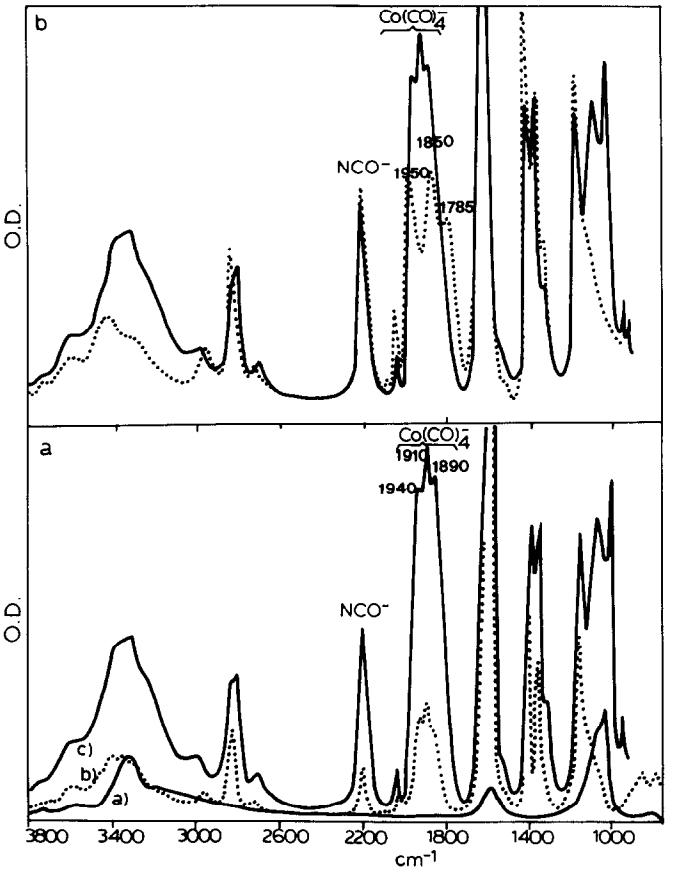

FIG. 5. (a) Spectrum a (—) IR spectrum for NH_3 (1 Torr) adsorbed on MC 3.4 solid solution; spectrum b (···) after dosing 40 Torr CO; spectrum c (—) spectrum of surface species obtained by directly dosing a 1/1 NH_3–CO mixture (P = 40 Torr) (spectrum taken after 6 h contact). (b) Effect of evacuation at room temperature on the IR spectrum of the adsorbed mixture (1/1): (—) before outgassing; (···) after outgassing for 5 min.

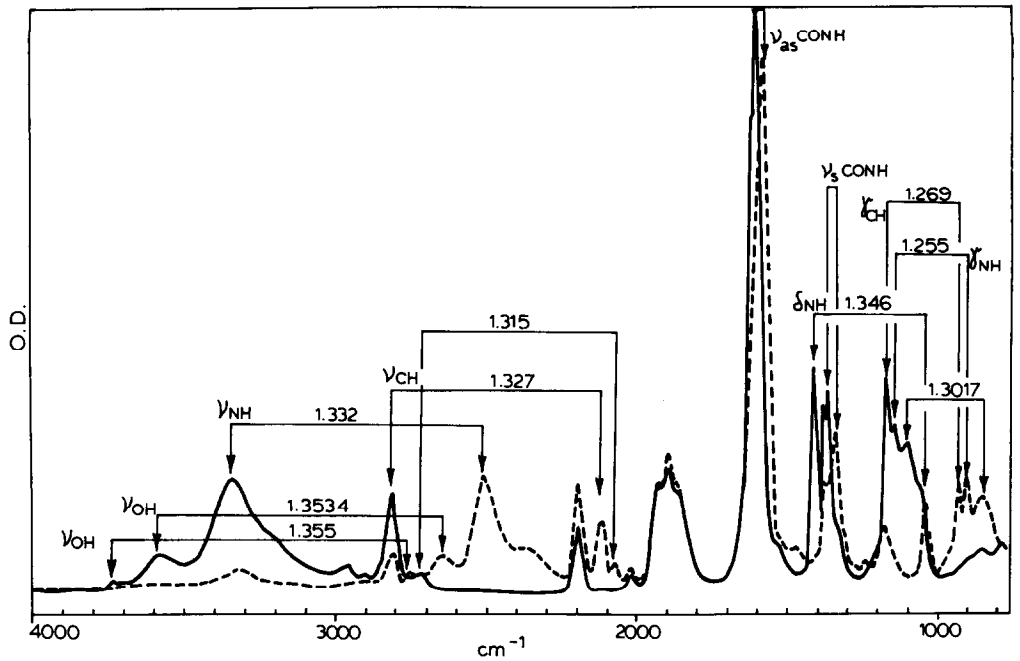

FIG. 6. IR spectra of CO–NH_3 (—) and CO–ND_3 (---) surface interaction products.

weakly adsorbed NH_3. If NH_3–CO interaction is carried out on pure MgO a similar IR spectrum is obtained, the main difference being the absence of the strong peaks at 2204, 2040, 1940, 1910, and 1890 cm^{-1}, which are so characteristic of the MgO–CoO solid solutions.

If the CO–NH_3 reaction is carried out on MgO–NiO solid solutions (results to be published), similar results are obtained. Also in this case the IR spectrum consists of two groups of peaks, one series characteristic of the MgO matrix and a second typical of the MgO–NiO solid solutions.

Due to the large variety of bands present on the MgO–CoO solid solutions after interaction between CO and NH_3, the assignment is troublesome. As the surface species come from NH_3 and CO, they contain presumably N, C, O, and H. In order to select the modes where the motion of hydrogen is involved, the spectra of surface products obtained from CO–NH_3 and CO–ND_3 interaction are compared in Fig. 6.

It can be seen that only the bands falling at 2204, 2040, 1940, 1910, and 1890 cm^{-1} are insensitive to deuteration; consequently, they belong to surface species not containing hydrogen and/or deuterium. On the contrary, all the other peaks move more or less downward; a plausible correlation scheme of the bands due to the same modes is reported in Fig. 6, where the isotopic ratios and the assignments are also reported.

The Spectra of the Py–CO Interaction Products

When CO is dosed on presorbed Py, new bands are observed at 2010(w); 1915(sh), 1890(s), 1875(sh), 1630(m), 1520(w), 1350(m), 1318(sh), 1215(sh), 1168(m), 1112(w), and 955(m) cm^{-1}, and the sample turns deep red (Fig. 4a). The peaks at 1350, 1168, and 955 cm^{-1} are absent when CO is dosed on pure MgO–CoO solid solutions.

Their behavior upon outgassing weakly adsorbed Py at RT is illustrated in Fig. 4b. It can be seen that (i) the peak at 1350 cm^{-1} moves slightly upward to 1353 cm^{-1}; (ii) the peak at 1168 cm^{-1} is not shifted; (iii) the band at 955 cm^{-1} shifts to 945 cm^{-1}; (iv) the quartet originally observed at 2010, 1915,

1890, and 1875 cm^{-1} is now observed at 2020, 1945, 1860, and 1800 cm^{-1}. Readsorption of Py restores the original spectrum; *consequently, the observed modifications are caused only by the presence or absence of weakly adsorbed Py.*

DISCUSSION

1. The Adsorption of NH_3

The bands at 3745, 3583, and 935 (irreversible to RT outgassing) can be assigned to the stretching (3745 and 3583 cm^{-1}) and bending modes (935 cm^{-1}) of surface hydroxyl groups. This assignment is confirmed by ND_3 adsorption experiments, which clearly shows a 1.35 isotopic ratio.

The presence of hydroxyl groups demonstrates that NH_3 heterolytically dissociates on the surface following the scheme:

$$O^{=}Me^{2+}O^{=} \xrightarrow{NH_3} \overset{NH_2^-}{Me^{2+}}OH^- \; ; \quad Me = Mg^{2+} \text{ and/or } Co^{2+} \qquad (a)$$

The stretching modes of the NH_2^- are at 3355 and 3250 cm^{-1}, while the bending mode is at 1557 cm^{-1} (because these bands are resistant to RT outgassing and thus belong to strongly adsorbed species).

The Co^{2+} ions involved in the dissociative process are those located on the edges and steps (and corners as well). The reflectance measurements show that NH_3 adsorption causes irreversible destruction of the 17,000-cm^{-1} peak already assigned to a *d–d* transition of Co^{2+} ions in distorted tetrahedral coordination (*1*). The high activity of the $Co^{2+}_{4C}O^{2-}_{4C}$ pairs (4C: fourfold coordinated) toward the heterolytic dissociation of hydrogen-containing molecules XH has been documented already (*2*). The capacity of MgO–CoO solid solutions to cause dissociation of the N–H bonds is also confirmed by the adsorption of NH_3–ND_3 mixtures. In fact, when a NH_3–ND_3 (1 : 1) mixture is dosed, four peaks at 1030, 960, 875, and 810 cm^{-1} are observed which are readily assigned to δ_s-modes of NH_3, NH_2D, ND_2H, and ND_3, respectively (*8*). The peaks of adsorbed NH_2D and ND_2H are the major components. This implies that the surface causes H/D equilibration, with the predominant formation of the statistically most probable NH_2D and ND_2H species. Of course, since the MgO matrix is also able to dissociate NH_3 (*5*), the observed isotopic equilibration results from the contemporary action of $Mg^{2+}O^{2-}$ and $Co^{2+}O^{2-}$ pairs. The occurrence of an H/D exchange reaction is also proved by the peaks at 1232, 1178, and 1150 cm^{-1} of Fig. 3 which are due to $\delta_a(ND_2H)$ (1232 cm^{-1}), $\delta_d(ND_3)$ (1178 cm^{-1}), and $\delta(ND_2^-)$ (1150 cm^{-1}).

Besides the RT irreversible peaks assigned predominantly to dissociatively adsorbed NH_3, the other pressure-sensitive bands monitor the presence of weakly adsorbed species. The presence of undissociated NH_3 is also proved by the weak narrow peaks at 4950 and 4250 cm^{-1} observed in the reflectance spectrum, which are undoubtedly due to overtones and combination modes of undissociated NH_3 (*8*).

The frequency values of the weakly adsorbed species observed on the solid solutions are similar to those found on the NH_3–MgO system (*5*); this implies that the vibrational modes of NH_3 adsorbed on Mg^{2+} and Co^{2+} ions have nearly identical frequency. This conclusion is in agreement with the similar ionic radius (and hence polarizing power) of the two ions. Besides the assignments and considerations presented in the paper dealing with the NH_3–MgO system (*5*), we only add here a few comments about the continuous frequency shift (with decreasing θ) of the $\delta_s(NH_3)$ modes at 1100–1000 cm^{-1}.

Continuous shifts (with θ) of the frequency of adsorbed species can be due to (i) dipole–dipole interaction (through the space dynamic effect); (ii) static interaction (through the solid chemical effect); (iii) static interaction through space (lateral interaction, for instance of the hydrogen bonding type).

Among the three mentioned effects, hydrogen bonding between molecules ad-

sorbed in adjacent positions cannot play the major role, not only because the coverage is not very high ($\theta \leq 0.2$) but also because it should cause (if operating alone) an upward shift of the $\delta_s(NH_3)$ mode.

Dipole–dipole interaction can also be excluded as the main effect responsible, since (i) it should cause an upward shift with increasing θ (in contrast with the experimental results) and (ii) it should be influenced by the isotopic composition of the mixture (in contrast with the behavior illustrated in Figs. 3b and c). It is therefore concluded that the observed shift is better explained by a static (through the solid) interaction. This effect can be described as follows.

NH_3 is adsorbed on Mg^{2+} and Co^{2+} ions through a weak dative bond, which having σ-donating character, increases the electron density on adjacent and more distance ions (the effect is thought to decay within a few spacings); consequently, as θ increases, the $Mg^{2+}(NH_3)$ and/or $Co^{2+}(NH_3)$ coordinative bond progressively becomes weaker, up to the limiting point where the state of the NH_3 molecule is becoming similar to that of a liquid-like phase. Indeed, the $\delta_s(NH_3)$ frequency progressively moves (as θ increases) from values typical of weakly coordinated NH_3 (*7*) to the value of the liquid state (*7*).

2. *The Adsorption of Py*

The bands of adsorbed Py (i.e., the Py which is resistant to RT outgassing) are typical of the Py nucleus σ-coordinated to weak Lewis centers (*7*). By comparison with the IR spectra of Py adsorbed on MgO (*6*) it is concluded that (as in the NH_3 case) Py molecules coordinated to Mg^{2+} and Co^{2+} ions have very similar IR spectra (as expected because Mg^{2+} and Co^{2+} have very similar σ-acceptor capacity).

However, the peak at 955 cm^{-1} cannot be ascribed to σ-coordinated Py, since (i) it develops gradually with time (i.e., it is formed in an activated process); (ii) unlike the other bands of σ-coordinated Py it is destroyed by O_2; (iii) a peak in identical position can be obtained when bipyridyl is directly dosed on the MgO surface (*9*); (iv) the growth of the peak at 955 cm^{-1} is parallel to the growth of the band at 24,000 cm^{-1} (already assigned to bipyridyl and polypyridyl radical anions) (*10*).

We therefore conclude that, as on MgO (*11*), on the diluted MgO–CoO solid solutions the following processes occur on the cobalt-free regions of the surface:

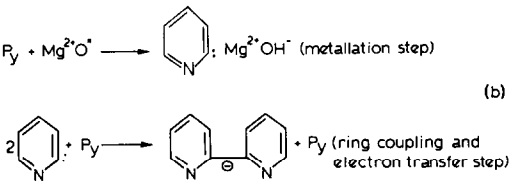

leading to bipyridyl and pyridine radical anions.

On the solid solutions the reducible character of the Co^{2+} ions must be taken into account as well because it will favor an alternative reaction pathway, which can be exemplified as

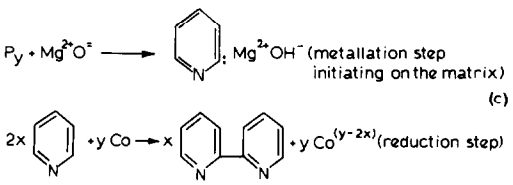

leading to the formation of neutral bipyridyl and cobalt in reduced state. This hypothesis justifies the experimental observation that when Py is left for several hours in contact with the solid solutions, an extensive formation of surface hydroxyl groups is observed which is absent or much weaker on pure MgO.

Unfortunately, the IR bands of the neutral bipyridyl cannot be detected because they are overshadowed by the similar (but much stronger) ones of adsorbed Py.

3. *The CO–NH_3 Interaction*

As on pure MgO (*11, 12*), NH_3 adsorbed on the cobalt-free areas of the matrix reacts with CO following the scheme

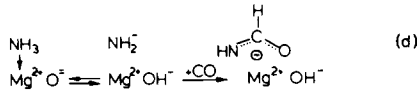

(d)

which justifies both the consumption of NH_2^- and of the weakly adsorbed NH_3 and the intensification of the OH^- species (because the equilibrium between the undissociated and the dissociated forms is shifted to the right).

Reaction (d) finds a precedent in organometallic chemistry. It is known that KNH_2 reacts with CO following the mechanism (*13*)

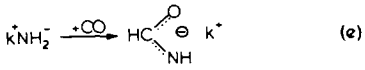

(e)

The presence of $HCONH^-$ groups after reaction with CO accounts well for the peaks at 3420 (ν NH); 2838 (ν CH); 1610 (ν_{as} —C(=O)NH); 1410 (δ NH); 1352 (ν_{sym} —C(=O)NH); 1160 cm^{-1} (γ NH).

The isotopic substitution pattern schematized in Fig. 6 totally confirms this assignment.

The two unusual peaks at 2955 and 2730 cm^{-1} are overtones of fundamental modes (1610 + 1352 and 1410 + 1352); this assignment is demonstrated by their opposite frequency changes upon NH_3 solvation (because the fundamental modes at 1352 and 1410 cm^{-1} move in opposite directions). The ν CH peak at 2838 cm^{-1} is also slightly perturbed by NH_3 adsorbed in adjacent positions (Fig. 5b) (downward 10-cm^{-1} shift and subsequent doubling of the peak).

Besides the bands of adsorbed $HCONH^-$, OH^-, and coordinated NH_3, intense peaks at 2204, 2040, 1910, and 1890 cm^{-1} are clearly observed which are totally absent on pure MgO. They belong to surface species which do not contain hydrogen because they are unaffected when ND_3 is used instead of NH_3.

On the basis of previous results obtained on the MgO–CoO system in the absence of preadsorbed NH_3, the quartet at 2040, 1940, 1910, and 1890 cm^{-1} is assigned to $Co(CO)_4^-$ species in distorted C_{2v} symmetry (*1*). The peak intensities and frequencies strongly depend upon the presence of molecularly adsorbed NH_3 (Fig. 5b) in the way fully discussed in Ref. (*1*). This effect can be briefly schematized as follows: NH_3 solvates the surface Mg^{2+} ions acting as positive counterions for the $Co(CO)_4^-$ entities with subsequent changes of the geometry of the cobalt carbonylate. In other words, $Co(CO)_4^-$ is less distorted in the presence of NH_3 (because the $Co(CO)_4^-$–Mg^{2+} pair is solvent separated) and more distorted in the absence of NH_3 (because the pair becomes a true contact pair). As has been completely demonstrated in Ref. (*1*), this effect can be quantitatively described in terms of changes of a distortion parameter and finds precedents in homogeneous chemistry.

The intensity of the bands of the $Co(CO)_4^{-1}$ anion are, however, much stronger in the presence of NH_3 (than in its absence). By comparison with literature data (*14*) and with previous results obtained by emission spectroscopy (*12*) the peak at 2204 cm^{-1} is assigned to NCO^- species. As the intensities of the NCO^- and $Co(CO)_4^-$ peaks grow with time in a parallel way, it is inferred that they owe their origin to the same surface process.

In the absence of presorbed NH_3, the $Co(CO)_4^-$ anions are formed following the scheme (*1*)

$$2Co^{2+} + 6\,O^= + 11\,CO \longrightarrow 2\,Co(CO)_4^- + 3CO_3^= \qquad (f)$$

which occurs on coordinatively unsaturated sites (such as edges and steps).

In the presence of NH_3 (and hence of $HCONH^-$) the following additional (alternative) mechanism is operating.

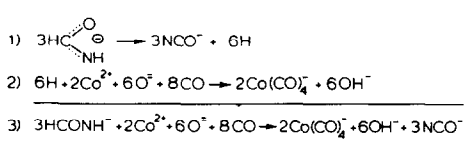

(g)

which is very similar to mechanism (f). Only the $HCONH^-$ species located on/or near to Co^{2+} ions are oxidized to NCO^-

species. The transformation of $HCONH^-$ species into NCO^- ones is well known in the organometallic chemistry of cobalt carbamoyl complexes (*13*).

We can see clearly here that doping MgO with Co^{2+} leads to oxidation of the $HCONH^-$ groups already at RT, with final formation of NCO^- species. This result can be achieved on pure MgO only by oxidation with O_2 at high temperature (*12*).

This result is important not only because it is an example of strict similarity between homogeneous and heterogeneous reactions, but also because it indicates how a controlled doping of MgO with Co^{2+} can selectively deviate the pathway of a surface reaction.

The usefulness of MgO–CoO solid solutions as model solids for surface investigations receives further support.

4. The CO–Py Interaction

This interaction readily causes the abundant formation of $Co(CO)_4^-$ anions (peaks at 2010, 1915, 1890, and 1875 cm^{-1}). As already discussed in Ref. (*1*), the frequency and the intensity of the $Co(CO)_4^-$ peaks is influenced very much by weakly adsorbed Py. The effect is similar to that described before for NH_3 and has received an identical explanation (*1*).

The Py-assisted formation of $Co(CO)_4^-$ anions is not unexpected, because we have seen before (vide supra) that Py acts as a reductant of surface Co^{2+} ions. By analogy with the NH_3 case, the whole process can be schematized as follows:

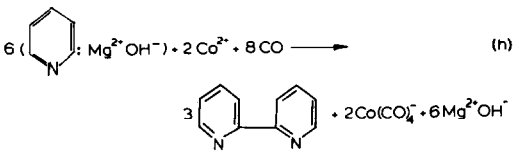

This process is similar to process (g); in fact, in both cases surface anions ($HCONH^-$ and $C_5NH_4^-$) are oxidized by Co^{2+} with subsequent formation (in the presence of CO) of $Co(CO)_4^-$ species.

In the presence of the CO–Py mixture other bands are also observed; among them the strongest ones are at 1350, 1168, and 955 cm^{-1}. As these bands are present (with higher intensity) when the same experiment is repeated on pure MgO, they must be ascribed to interaction products formed on cobalt-free portions of the surface and thus will be discussed thoroughly in a subsequent paper to be entirely devoted to the Py–CO interaction on MgO (*15*). We anticipate that they are associated with polymeric $(CO)_n^{x-}$ species formed during a process similar to that described in Ref. (*16*).

ACKNOWLEDGMENT

This work was carried out with financial support from the Consiglio Nazionale delle Ricerche, Progetto Chimica Fine e Secondaria.

REFERENCES

1. Zecchina, A., Spoto, G., Coluccia, S., and Guglielminotti, E., *J. Phys. Chem.* **88,** 2575, 2582, 2587 (1985).
2. Zecchina, A., and Spoto, G., *Z. Phys. Chem. (Munich)* **137,** 173 (1983).
3. Zecchina, A., Spoto, G., and Coluccia, S., *J. Mol. Catal.* **14,** 351 (1982).
4. Cordischi, D., Indovina, V., Occhiuzzi, M., and Arietti, A., *J. Chem. Soc. Faraday Trans. 1* **75,** 533 (1979).
5. Coluccia, S., Garrone, E., and Borello, E., *J. Chem. Soc. Faraday Trans. 1* **79,** 607 (1983).
6. Coluccia, S., and Zecchina, A., in press.
7. Morterra, C., Chiorino, A., Ghiotti, G., and Garrone, E., *J. Chem. Soc. Faraday Trans 1* **75,** 271 (1979).
8. Reding, F. P., and Hornig, D. F., *J. Chem. Phys.* **11,** 514 (1951).
9. Coluccia, S., Garrone, E., and Morterra, C., *Z. Phys. Chem. (Munich)* **124,** 201 (1981).
10. Zecchina, A., and Stone, F. S., submitted for publication.
11. Garrone, E., and Stone, F. S., *in* "Proceedings, 8th International Congress on Catalysis, Berlin, 1984, Vol. III p. 441. Verlag Chemie, Weinheim, 1984.
12. Borello, E., Coluccia, S., and Zecchina, A., *J. Catal.* **93,** 331 (1985).
13. Behrens, H., *Adv. Organomet. Chem.* **18,** 1 (1980).
14. Nakamoto, K., "Infrared Spectra of Inorganic and Coordination Compounds." Wiley, New York, 1970.
15. Guglielminotti, E., and Zecchina, A., in press.
16. Guglielminotti, E., Coluccia, S., Garrone, E., Cerruti, L., and Zecchina, A., *J. Chem. Soc. Faraday Trans. 1* **75,** 96 (1979).